Segmentation of Brain MRI Using Active Contour Model

Amira Ben Rabeh, Faouzi Benzarti, Hamid Amiri

National Engineering School of Tunis (ENIT), Signal, Image and Technology Information (LR-SITI), Manar, Tunisia

Received 26 April 2016; revised 28 October 2016; accepted 5 December 2016

ABSTRACT: Alzheimer disease is a neurodegenerative disorder that impairs memory, cognitive function, and gradually leads to dementia, physical deterioration, loss of independence, and death of the affected individual. In this context, segmentation of medical images is a very important technique in the field of image analysis and Computer-Assisted Diagnosis. In this article, we introduce a new automatic method of brain images' segmentation based on the Active Contour (AC) model to extract the Hippocampus and the Corpus Callosum (CC). Our contribution is to combine the geometric method with the statistical method of the AC. We used the Caselle Level Set and added a learning phase to build an average shape and to make the initialization task automatic. For the step of contour evolution, we used the principle of Level set and we added to it the a priori knowledge. Experimental results are very promising. Int J Imaging Syst Technol, 27, 3–11, 2017; Published online in Wiley Online Library (wileyonlinelibrary.com). DOI: 10.1002/ima.22205

Key words: Alzheimer disease; computer-assisted diagnosis; hippocampus; corpus callosum; active contour

I. INTRODUCTION

Alzheimer's disease is a neurodegenerative disorder that impairs memory and cognitive function. It is divided into three main phases: the Mild Cognitive Impairment (MCI) stage, the moderate stage, and the severe stage. At the mild stage, the person is usually able to think appropriately, and to make crucial decisions about future; However, Some negative symptoms are remarkable during this stage such as forgetfulness and communication problems, for instance, finding the right word or following a conversation. In the moderate stage, there is a further deterioration of mental and physical abilities of the person. Memory loss worsens. One can no longer remember his/her personal history and can no more recognize his/her family and friends. In the severe stage, the person is no longer able to remember anything, communicate with anyone, or even take care of oneself. The patient will require a special care day and night. This disease can be genetic, but that is not the primary cause of degenerative dementia. The latest statistics show that there are 12 million patients worldwide. This number keeps growing and the forecast estimates 18 million cases in 2025. In Tunisia, the number is alarming: about 30 000 people are affected, to 1.5 million in the Arab world. The elderly are the most affected, but the dementia is striking more and more young people. What constitutes a prime therapeutic challenge is the fact that no current treatment can permanently eradicate the disease. (Aminoff et al, 2007; Bar et al, 2003; Bear et al, 2007; Bollinger et al, 2011; Buckner et al , 2008; Dickerson et al, 2009; Epstein et al, 1999). In fact, it is very important to go through an image processing to detect and locate the affected area. The image segmentation is one of the techniques that can bring about some crucial information for diagnostic assistance. It is defined as the process of partitioning a digital image into multiple segments or regions.

The diversity of images, the difficulty of the problems, the researchers' varied origins, the evolution of computers, as well as certain empiricism in the evaluation of results led to the introduction of a multitude of algorithms. The reliable and accurate segmentation of anatomical volumes whether normal or pathological from imaging systems aims at developing the medical diagnosis because it may help studying morphology internal structures, and it may help the detection and quantification of the lesions. Many segmentation methods have been proposed for many years for the MRI type of images. The automatic brain MRI segmentation is a complex problem from the point of view of the variability of the human brain in terms of images processing acquired by this method. Brain MRI segmentation is an essential basic step that has many applications in neurology such as quantitative analysis, operational planning, and functional imaging. Although very accurate to describe the structures of the brain, magnetic resonance images present many difficulties like low contrast and inhomogeneity, but their treatment can be achieved through simple approaches. In this work, we suggest a new automatic method of segmentation based on the Active Contour (AC) model.

This article is organized as follows. In the following section, we present some related works. In the third section, we present the suggested method. In the last section, we give some experimental results, and a discussion.

II. RELATED WORKS

There are many methods for segmentation of the Brain MRI, such as:

A. ASM + D Proposed by (Said Taieb et al., 2014). This method proposed by Said Taieb et al. (2014) to extract the

Correspondence to: Amira Ben Rabeh; e-mail: amira.benrabeh@gmail.com

Hippocampus using the static model: ASM (Active Shape Model) this method of segmentation is based in the priori knowledge. He used the distance between the two hippocampus as a priori knowledge.

B. Method Proposed by (Kayalvizhi et al., 2013). This method proposed by Kayalvizhi et al. (2013), he analyzed MRI brain images: coronal section weighted T1 and studied the progression of severity in Alzheimer's disease conditions. He used the geometric model Level Set.

C. Method Proposed by S. Matoug. As a solution, he introduced an automatic tool in 2011 that reads volumetric MRI and performs two-dimensional volume slices and volumetric segmentation methods to segment gray matter, white matter, and cerebrospinal fluid. For segmentation, he used the parametric model Snake.

III. PROPOSED METHOD

We used the MRI data sets database from the Open Access Series of Imaging Studies (Ardekani and Bachman, 2009).

Our contribution is based on:

a. Preparation of a learning phase to extract an average shape and automatic position of this form.
b. Improvement at the stage of the deformable model evolution. We incorporated a priori knowledge of the surface and the standard deviation.

Overall model: we will integrate a priori knowledge of surface and deviation of the studied area (Fig. 1).

A. Learning Phase. The objective is to learn the geometry and the variations in the structure that it is desired to locate later. Therefore, it seeks to establish a model that describes the shape and typical fluctuations. This first step requires the preparation of a learning database reflecting possible variations in shape of this structure.

A.1. Average Shape and Automatic Position. **Preparation of the learning base** The preparation of a training base for a given structure is to initially collect a sample image database reflecting possible variations in its shape. For that, the constructed model would be sufficiently representative, the number of images collected should be relatively high and instances of quite varied shapes should be selected. Then, we extract the shapes from the sample images on each image by placing a sufficient number of characteristic points. These points should be placed carefully on the contour of the structure studied to clearly represent its details. The points, which are defined by an expert, provide a precise meaning. In fact, each form will be modeled by a vector × constructed by concatenation of the coordinates of characteristic points located on the outline:

$$x=(x1,\ x2,\ldots\ldots\ldots,\ \mathrm{xn}) \tag{1}$$

The training set can be modeled by a set of vectors:

$$\{\mathrm{xi}\}\ \text{avec}\ i=1\ldots N\ (N\ \text{number of sample images})$$

Forms alignment The extracted forms during the previous step are independent of the parameters of size, and position. There may have shapes, which are more or less remote in different directions and have different sizes. However, the modeling approach is to study only the essential shape variation between the different configurations of the studied structure. Thus, to solve this problem of variation of size and position of the N forms of the training set, the contours must be aligned with one of the obtained contours. This will be used as a reference.

The alignment procedure is to first take a random form which is aligned with all others. Then, at each iteration, an average shape is calculated, and normalized on the other which will be realigned. This process is stopped when the average form reaches a certain criterion. It is supposed to converge regardless of the initial form chosen.

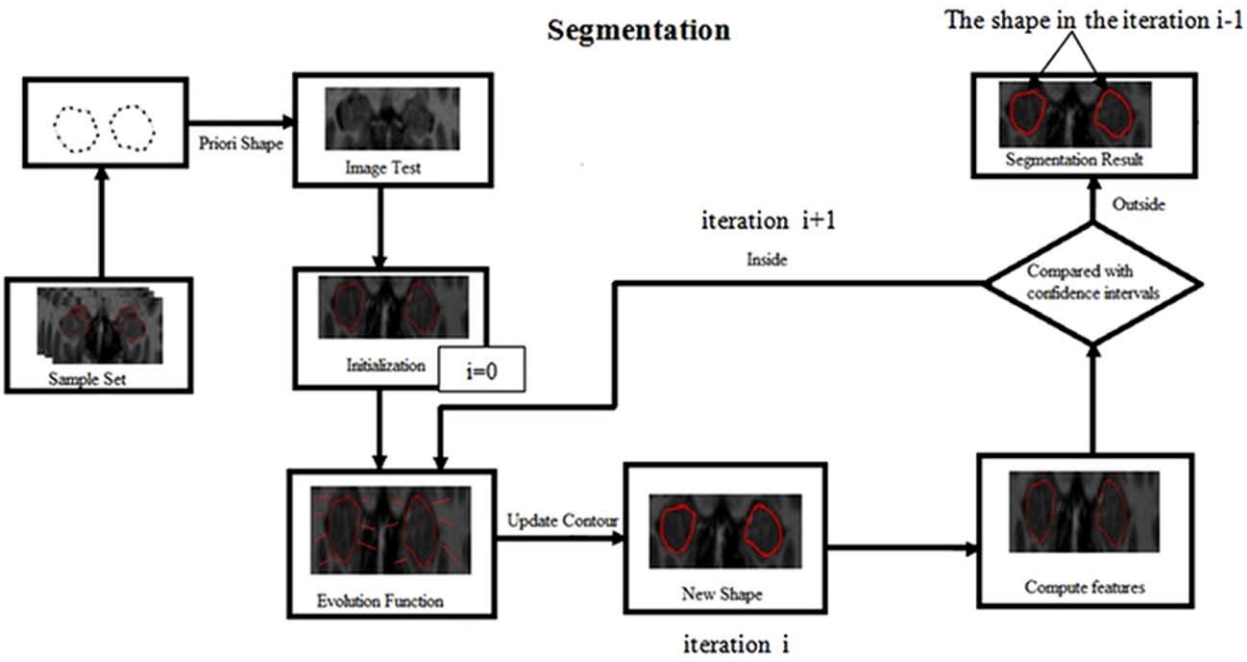

Figure 1. Overall model. [Color figure can be viewed at wileyonlinelibrary.com]

Generation of the average shape The aligned vectors, resulting from the previous two steps can be arranged as a matrix of size (2*n*, *N*), called the observation matrix. The columns correspond to shapes and lines correspond to the coordinates of the characteristic points describing each shape.

This can be done by examining the variation of homologous characteristic points on all forms. If we consider, for example, the first two lines of the observation matrix, they represent the coordinates of the first feature point through different forms. By examining the change in these coordinates and passing from one form to another, one can deduce the path followed by this point and the amplitude of variation. However, the problem is that each form is represented by n feature points, each identified by its coordinates (*x*, *y*) in the plan. Therefore, for a single point, we used 2*N* variables and for all the points, we used 2*nN* variables. To simplify the problem and reduce the number of variables that describe each shape, the idea is to apply a principal component analysis (PCA) on the raw data.

In practice, the main components are derived from the covariance matrix associated with the observation matrix. To determine the mode of variation of a shape, we can simply compare this shape with respect to an average computed shape, instead of comparing with all other forms. This comparison is between the coordinates of points as characteristics compared with counterparts in average shape. The deviation of the *i*th shape with respect to the average shape may be defined by the expression:

$$dxi=(x_{i1},y_{i1},x_{i2},y_{i2},\ldots,x_{\mathrm{in}},y_{\mathrm{in}})-(\overline{x_1},\overline{y_1},\overline{x_2},\overline{y_2},\ldots,\overline{x_n},\overline{y_n})=\mathrm{xi}-\overline{x} \tag{2}$$

When $\overline{x}=\frac{1}{N}\sum_{i=1}^{N} xi$, the average computed shape from the learning base aligned.

Automatic initialization of the average shape Our first contribution is to overcome the stage of manual initialization. In this way:

$$M=\begin{pmatrix} X1Y1 \\ X2Y2 \\ \ldots\ldots\ldots \\ \ldots\ldots\ldots \\ \ldots\ldots\ldots \\ XNYN \end{pmatrix}=\begin{pmatrix} p1 \\ p2 \\ \ldots.. \\ \ldots.. \\ \ldots.. \\ pN \end{pmatrix} \tag{3}$$

$N = n*N\mathrm{ech}$

n: number of points that have the outline of an image.

*N*ech: number of samples

The M matrix is of dimension $N * 2$

Through this matrix, the average position is determined by:

$$P\mathrm{osm}=\frac{1}{N}\sum_{i=1}^{N} pi \tag{4}$$

A.2. Priori Knowledge of the Surface. Each image is recorded by the surface of the studied form by using Eq. (5):

$$Si=\sum_{i=1}^{nbl}\sum_{j=1}^{nbc} Xij \tag{5}$$

Xij: the pixel is in the iem row and column jem.

$$V\mathrm{s}=(S1,S2,\ldots,\mathrm{Sn})$$

The average surface of interest structures

$$Sm=\frac{1}{n}\sum_{i=1}^{n} Si \tag{6}$$

- The variance, which measures the dispersion of the elementary surfaces (*Si*) relative to the average surface:

$$V(s)=\frac{1}{n}\sum_{i=1}^{n}(\mathrm{Si}-\mathrm{Sm})^{2} \tag{7}$$

- The standard deviation, which represents the average of all deviations; basic variances compared with the average distance:

$$\sigma=\sqrt{V(s)} \tag{8}$$

Then, we will propose a confidence interval $[Sm-2\sigma, Sm+2\sigma]$.

For each iteration, we calculate the surface of the area. If the surface is lower than the lower limit of the interval, we stop the evolution of the curve.

A.3. Priori Knowledge of Standard Deviation. Each image is recorded by the variation of the studied area.

We integrate the prior variance. We search the average, the variance, and the standard deviation of the variance of form.

$$V\mathrm{ars}=(V\mathrm{ar}1,V\mathrm{ar}2,\ldots,V\mathrm{arn}) \tag{9}$$

Constructing a vector contains all the variations of the areas of the hippocampus of the samples of the base.

The average change in interest structures:

$$V\mathrm{arm}=\frac{1}{n}\sum_{i=1}^{n} V\mathrm{ari} \tag{10}$$

The variance, which measures the dispersion of elementary variations (*Si*) relative to the average variation.

$$V(var)=\frac{1}{n}\sum_{i=1}^{n}(Vari-Varm)^{2} \tag{11}$$

The greater the variance is, the more heterogeneous the appropriate area (hippocampus) is. The standard deviation, which represents the average of all deviations basic variances compared with the average distance.

$$\sigma=\sqrt{V(var)} \tag{12}$$

Then, we will propose a confidence interval $[V\mathrm{arm}-2\sigma, V\mathrm{arm}+2\sigma]$.

The goal is to derive a compact formulation describing the permitted variance. In fact, from *V*ars, we can calculate the parametric statistics. The basic idea is if there is a level change out of range, it offers the inverse of the curve. The curve evolves internally instead of the convergence towards the outer neighbor pixels.

B. Segmentation. *B.1. Development of Method.* Statistical method (based on priori knowledge) and geometric method (The evolution of the curve based on neighbored pixels). In the following sections, we will first introduce each method apart and then, we will explain why and how we combined the two of them (Aljabar et al., 2009; Atif et al., 2006; Ardekani et al., 2009; Delingette et al., 2001; Duvernoy et al., 2005).

B.2. Geometric Deformable Models. The geometric models provide an implicit representation of the curve as the zero level of a scalar function of higher dimension. The move towards the target contour is based on the evolution of curves theory, which only depends on the intrinsic geometric properties. These properties are the standards defining the direction of evolution and the curve defining the velocity at each point. Thus, no functional energy is used, and therefore no programming is considered.

Level set The Level Set method was originally introduced by Osher and Sethian. This method allows changing a curve implicitly defined as the zero level of a higher order function to the target curves in the image. Changes can be made according to several criteria. The formulation of this method, where the change is based on the average intensities inside and outside of the curve, is well suited to the detection of homogeneous regions having no sharp boundaries. It is also more robust in the presence of noise.

The level set model (Level set) suggests an interesting analytical framework for geometric curve evolution through the implicit representation. It describes the curve as the zero level of a scalar function of ϕ higher dimension levels, instead of using a conventional parametric representation. The function of ϕ levels will be defined in the image plan and will evolve over time in the direction of normality and with a speed of propagation. Therefore, the spread (zero curve) will be detected easily from that of ϕ. The latter is defined as a signed distance between any point of the image and the curve:

$$\begin{gathered}\phi : R^2 \to R \\ \phi(\mathrm{x},\mathrm{y},\mathrm{t}) = \mp d((\mathrm{x},\mathrm{y}), v) \\ \phi(\mathrm{x},\mathrm{y},\mathrm{t}) = 0 : si(\mathrm{x},\mathrm{y}) \in v \quad \text{Distance from}(x,y)\,\text{to}\,v\end{gathered} \tag{13}$$

The initial curve V_0 is defined by points such as: $\phi(\mathrm{x},\mathrm{y},\mathrm{t}=0)=0$

The evolution equation of the curve Vthrough the function ϕ is defined by:

$$\frac{\partial \phi(\mathrm{v},\mathrm{t})}{\partial t} + F(k)\,|\nabla \phi(\mathrm{v},\mathrm{t})| = 0 \phi(\mathrm{v},\mathrm{t}=0) \tag{14}$$

During evolution, all forms represented by the curves can be defined by:

$$\{(\mathrm{x},\mathrm{y}) / \phi(\mathrm{x},\mathrm{y},\mathrm{t}) = 0\} \tag{15}$$

With this implicit representation, this model provides an opportunity to change the topology, and thus the detection of multiple contours from a single initial curve. However, the numerical implementation of the $\varnothing$ level function is very time-consuming. Indeed, the evaluation of $\varnothing$ involves estimating local features (normal curvature) at any point of the image. Several other similar models, using an implicit representation of the curve and adopting geometric constraints for evolution have been proposed. This implicit representation explains all the success of this class of geometric models. Indeed, the theoretical results have shown the existence and the uniqueness of the solution, which depends on few parameters.

In addition to that, they allow to detect several contours at a time and this takes the same amount of time as for the calculations of the $\varnothing$ level function. However, despite their advantages, these models have limitations. First of all, they are only valid for closed curves, which greatly limits their use. Then the resolution procedure is rather difficult to implement, compared with parametric models. (Caselles et al., 1997; Chan and Vese, 2001; Charmi et al., 2008; Chen and Radke, 2009).

B.3. Statistical Deformable Models. The ASM is a variation of statistic deformable models, introduced by Cootes and Taylor (1994) to extract objects complex and not rigid. The advantage of the ASM compared to other variants of deformable models lies in the fact that the evolution of the curve is guided by a strong a priori knowledge about the geometry and structure of the deformation modes studied. This knowledge is represented by a statistical model, which form describes a space of allowed deformations. The construction of such a model is made by applying a PCA on a learning base, which includes the various possible forms of the object.

These models provide a discrete representation of the curve by a set of feature points. They are based on a preliminary statistical analysis of the variations of the designed structure. The implementation of a statistical model then requires the preparation of N representative examples of the object under study and the priori knowledge. The shape of the object in each case is modeled by a vector of feature points x. Then, an average shape $\overline{x}$ supposed to be a relevant representative of all forms is deduced:

$$\overline{x} = \frac{1}{N} \sum_{i=1}^{N} xi \tag{16}$$

By applying a PCA on the average shape $\overline{x}$. Patterns and magnitudes of deformation of the object studied are detected. Thus, a particular form x can be simply expressed in terms of the average shape and a linear combination of the principal modes of deformation:

$$x = \overline{x} + \phi b \tag{17}$$

When $\phi = (\phi_1, \phi_2, \phi_3, \ldots \phi_t)$ is an orthogonal basis set by the modes of t the most significant deformations (principal components).

$b = (b_1, b_2, b_3, \ldots b_t)^t$ Represents the projection of a form x in this base. By varying the parameters, new forms similar to those obtained in the learning phase can be generated. Therefore, an area of authorized forms can be defined by properly limiting parameters:

$$-b_{\max_i} \leq b_i \leq b_{\max_i},\ i = 1 \ldots t \tag{18}$$

The final outline, describing the shape of the target object, must belong to this space. In the localization process, the evolution of the initial curve (which is usually the average shape) is done through a strategy using local intensity of the image. This development can be done in the space of predefined authorized deformations.

The ASM tenders ability to integrate a strong knowledge very effectively prior shape on the structures of interest. It is based on statistical models of shape structures designed to guide the segmentation step. This reduces solutions space and always lead to correct forms (Andreopoulos et al., 2008; Aymeric et al., 2005; Babalola et al., 2009; Bascle et al., 1994).

B.4. Fusion of the Two Models. In the learning step, we used the principle of the Statistical model; we used n patterns and we determined the average shape and the average position. In addition,

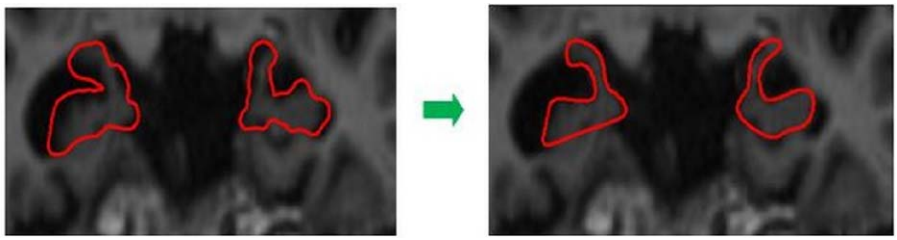

Figure 2. Improvement using variation. [Color figure can be viewed at wileyonlinelibrary.com]

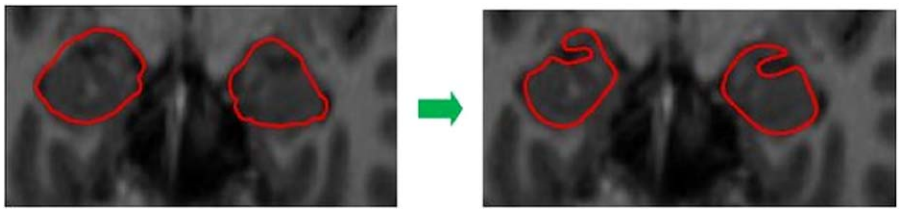

Figure 3. Improvement using surface. [Color figure can be viewed at wileyonlinelibrary.com]

we calculated the two confidence intervals to integrate the priori knowledge.

For the evolution of the curve, we used the principle of the geometric model: evolution of the curve based on neighbored pixels.

We combined the two models, the geometric and the statistical to integrate the priori knowledge to the geometric model, and therefore, the segmentation method will be automatic. The objective of the two models fusion is to improve the segmentation quality. The curve can converge towards other homogeneous areas with the studied area. Integrating the priori knowledge of the surface, we can improve the limit. The curve can converge towards other inhomogeneous areas with the studied area via integrating the priori knowledge of the variation. We can improve the limit of the segmentation.

Basic algorithm Once the learning phase is done, we get two confidence intervals: For each iteration, we extract the area studied (Hippocampus or the Corpus Callosum, CC) from contour. Then, we calculate the surface. If the surface is included in the interval, we follow the daily evolution, otherwise if the surface exceeds the upper bound, the evolution stops. We calculate the variation of the studied area. If the variation exceeds the upper limit, the daily changes are reversed, so the curve evolves internally instead of converging toward the outer neighbor pixels.

Using the constraint of the variation to improve the limit by the figures below: the contour may include the hippocampus more areas surrounding it and that are not homogeneous with the desired area. Through the confidence interval of variation and a priori knowledge, these limitations can be overcome (Fig. 2).

The constraint of the surface is used to improve the limit by the figures below: the contour may include the hippocampus more areas surrounding it and that are homogeneous with the desired area. Through the surface of confidence interval and a priori knowledge, these limitations can be overcome (Fig. 3).

The algorithm in below presents the principle of our method:

Input After the step of the training:

- We determine the two confidence intervals of the Surface and the variation.
- We determine the average shape and the initial curve.

Body We launch the initial curve.

For each iteration, calculating the surface and the variation:

If the surface is higher than the upper limit of the interval:

- Inverse the changing curvature. (To ensure that the outline does not converge to other areas that appear to be consistent with the area studied) and stop the evolution of the curve.

If the surface is in the range of trust:

- The daily evolution is kept.

If the variation exceeds the upper range of the confidence interval:

- A reverse development is provided, the curve changes internally instead of converging toward the outer neighbor pixels.

Output We find the final curve and we extract the correct area.

IV. EXPERIMENTAL RESULTS

We are interested to extract the two areas: Hippocampus and Corpus Callusm. We used three subjects: normal, suffering from Alzheimer's disease in the early stage and another in an advanced stage. We used the two sections frontal and sagittal for any subjects. We segmented the hippocampus of the three subjects by four methods: parametric model (snake; Charmi et al., 2008), static model (ASM; Cootes and Taylor, 1994), geometric model (Level Set; Caselles et al., 1997) and the fourth method is our proposed method Modify Level set which is a combination between the static and geometric models. We show the results in the figure below (Fig. 4).

Using our method Modify Level Set, we can calculate some features of geometries such as surface, perimeter, and standard deviation. We present in the table below the measurement of the features for the two parts of hippocampus (Tables I and II).

A.1. EXTRACTION OF THE CC

We segmented the CC of the three subjects by four methods (Fig. 5).

In reviewing the results: for lines 3, 4, and 5, we note that the curve migrates to similar intensity regions and sometimes not. For

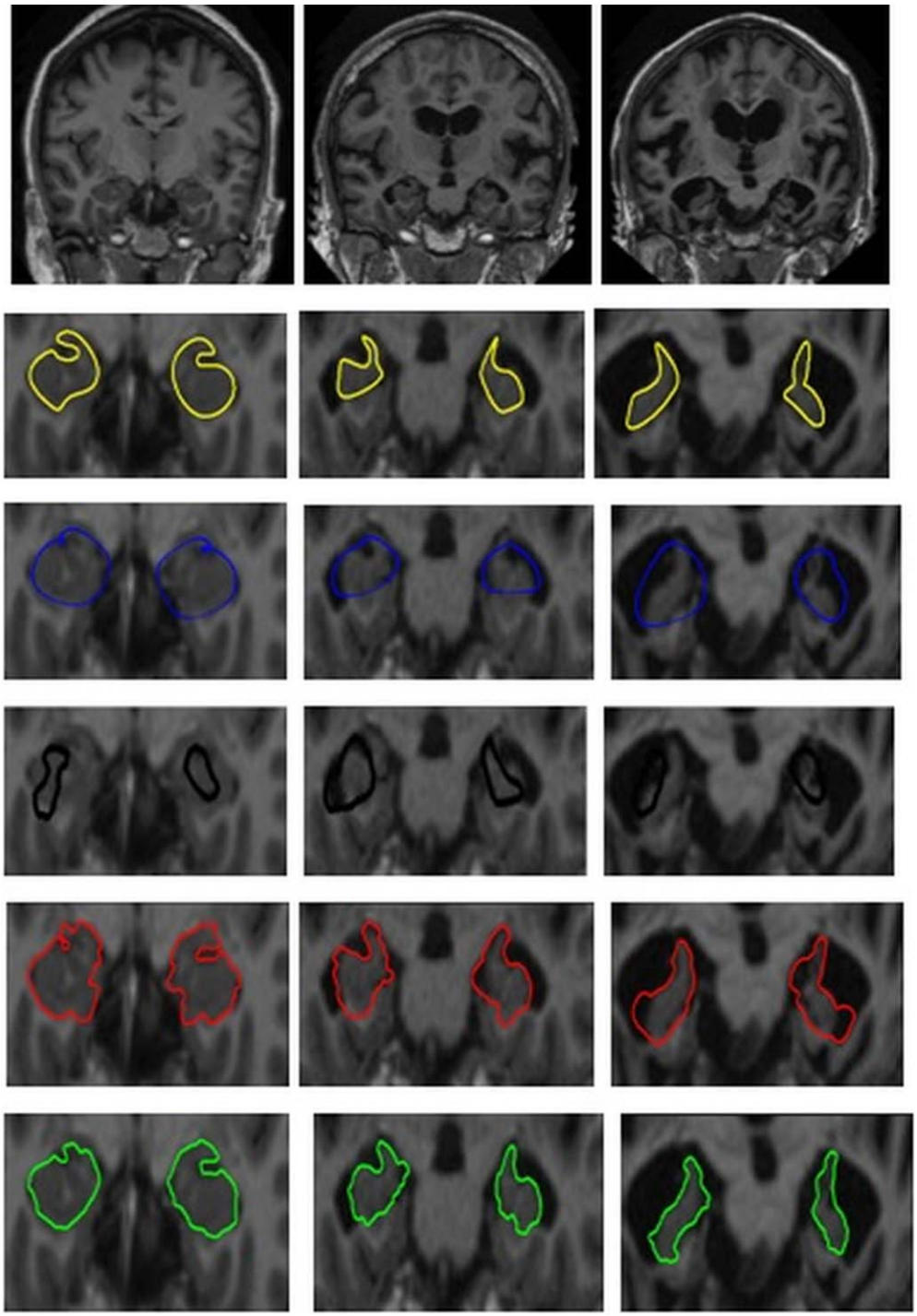

Figure 4. Results of the segmentation of the hippocampus. The six lines present in order: initial image, image manually segmented, the result using the snake method (parametric model), the result using the ASM method (statistical model), the result using the method Level Set (geometric model), the result using the Modify Level Set method (geometric model + Statistics). Column 1 shows a normal subject, column 2 about Alzheimer (primary stage) and the third column corresponds to an Alzheimer's subject (advanced stage). [Color figure can be viewed at wileyonlinelibrary.com]

Table I. Table of measurement for the hippocampus.

	Hippocampus L			Hippocampus R		
	Surface	Perimeter	Standard Deviation	Surface	Perimeter	Standard Deviation
Subject 1	1039	174.61	7	1425	170	8.3
Subject 2	1019	166	14	1267	160	17
Subject 3	902	155	17	1111	151	18.7

Table II. Table of measurement for Corpus Callosum.

	Surface	Perimeter	Standard deviation
Subject 1	5518	687	7.4
Subject 2	5173	658	17
Subject 3	3435	645	19

the 6th line, we can see that the curve evolves maintaining more regular results. It happens to capture the shape of the target structure.

In our case, we have three topics, segmented manually by a nuclear medicine department radiologist Kassab Hospital of Tunis. We will use this data to make a quantitative assessment of the proposed model.

We integrated the a priori knowledge with the geometric model. We decided to compare our model Modify Level Set, the

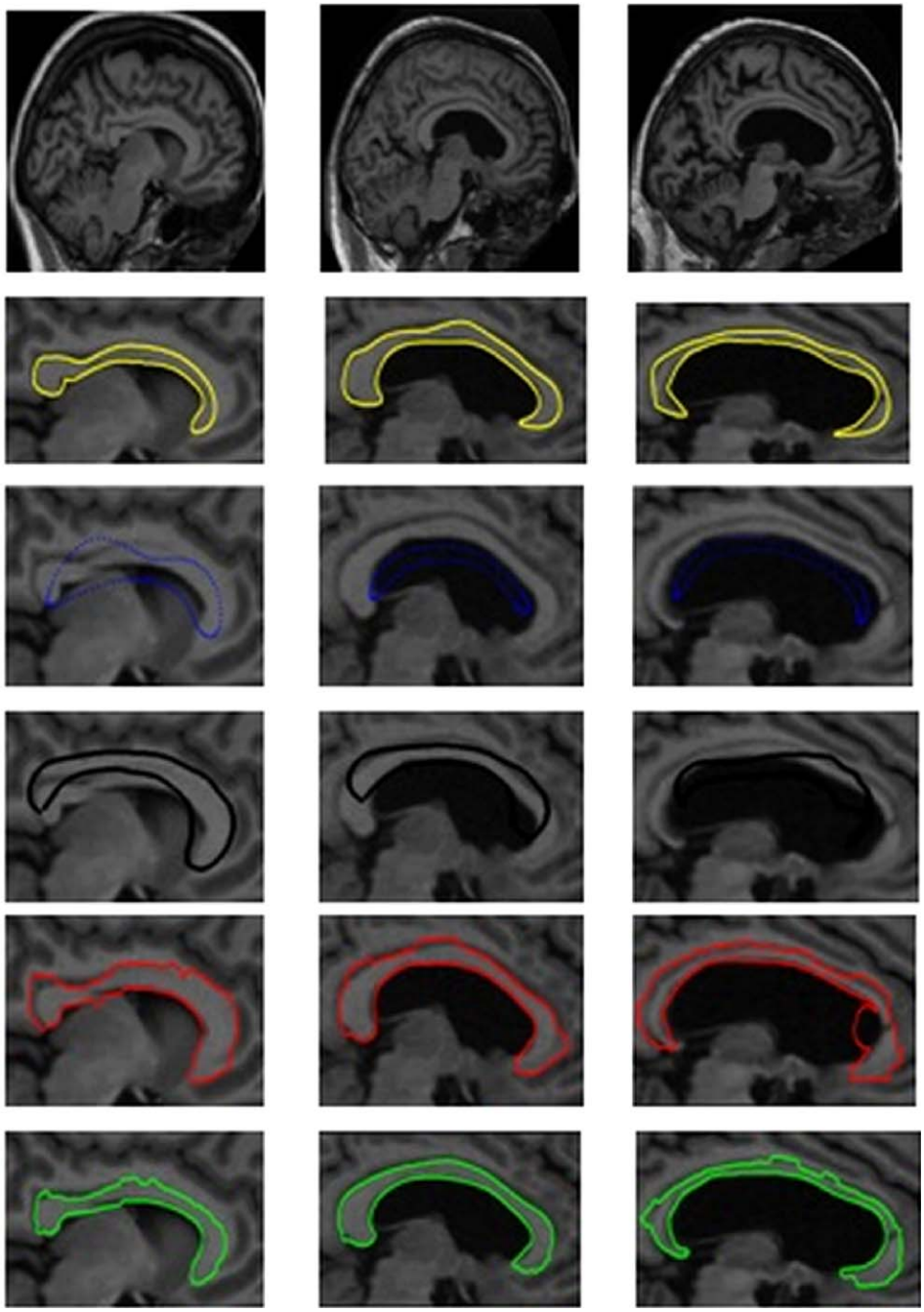

Figure 5. Results segmentation corpus callosum. The six lines present in order: initial image, image manually segmented, the result using the snake method (parametric model), the result using the ASM method (statistical model), the result using the method Level Set (geometric model), the result using the Modify Level Set method (geometric model + Statistics). Column 1 shows a normal subject, column 2 about Alzheimer (primary stage) and the third column corresponds to an Alzheimer's subject (advanced stage). [Color figure can be viewed at wileyonlinelibrary.com]

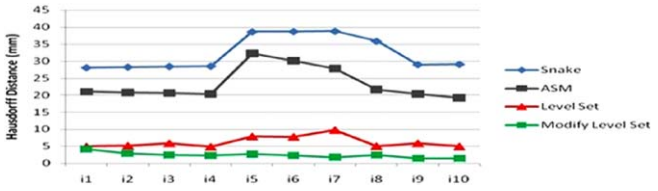

Figure 6. The figure shows the results of calculating the Hausdorff distance between the four methods (Modify Level Set, Level Set, ASM, and Snake) compared with the ground truth for the normal subject based on iterations. [Color figure can be viewed at wileyonlinelibrary.com]

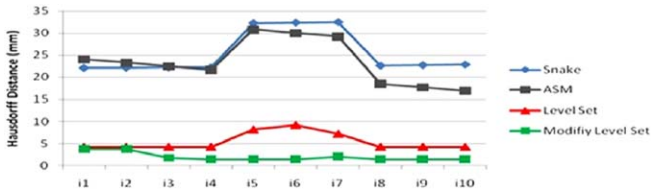

Figure 7. The figure shows the results of calculating the Hausdorff distance between the four methods (Modify Level Set, Level Set, ASM, and Snake) compared with the ground truth for the MCI subject based on iterations. [Color figure can be viewed at wileyonlinelibrary.com]

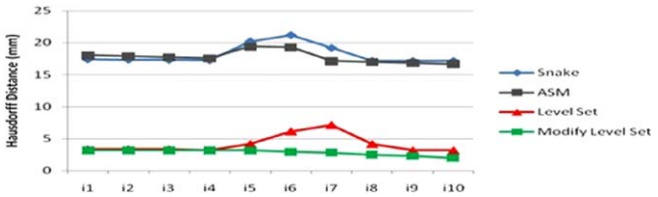

Figure 8. The figure shows the results of calculating the Hausdorff distance between the four methods (Modify Level Set, Level Set, ASM, and Snake) compared to the ground truth for the Alzheimer subject based on iterations. [Color figure can be viewed at wileyonlinelibrary.com]

original geometric model Level Set, statistical model ASM and the method based on parametric AC (Snake) with the ground truth.

The four methods are based on the deformable contour; we chose the Hausdorff distance as a measure of quality of segmentation. This metric is widespread in the medical field and admits multiple applications. In our case, we will use this distance to measure the degree of similarity between two geometric shapes (Figs. 6–8).

V. DISCUSSION

Examining the three diagrams, we can clearly see that the green curve shows some stability compared with the other curves; the blue, the gray and the red. In fact, for the green line in the three diagrams, the values of the Hausdorff distance are between 1,41et 4.12 (mm).In contrast, for the other three curves, the values of the Hausdorff distance often show large variations, which rose from 4.26 to 38.72 mm.

The poor performance of the ASM model and the SNAKE model can be explained by the vagueness of the initialization in some pictures of the sequence and the generality of the prior information of the used form.

Another interesting finding is that the value of the Hausdorff distance, such as Level Set, Modify Level set, or SNAKE compared with manual segmentation, varies considerably from one sequence to another. For example, in the Figure 6 this distance exceeds 23 mm for ASM and the SNAKE while in Figure 8 this distance does not exceed 16 mm. This may be related to the quality of the processed sequence, which influences the result.

Through these measures, although in some cases the ASM model, the model SNAKE provide more or less acceptable results, we can see that our model for each sequence provides a more stable and comprehensive income closer to the manual segmentation. This can reveal the importance of the integration of a priori knowledge with the geometric model.

In this work, we presented a segmentation method based on Level Set formalism coupled with a priori knowledge of the form. This work is part of the same knowledge integration problem a priori to improve segmentation results.

Indeed, we have introduced two points value in the segmentation process:

- The initial zero level curve is calculated from the average shape of the structure to be segmented. It will be more close to the target structure when locating.
- The change is limited to an allowed deformation field predefined. This reduces space solutions and always result in eligible forms.

This is what has led to promising segmentation method, which was applied for segmentation of internal brain structures in MRI images. That shows that the contributions of the integrated form of statistical constraint improve the accuracy of results.

In conclusion, it is clear that the integration of a priori knowledge of the area and the changes of the shape of the hippocampus had significantly improved results for the segmentation of image sequences. This is what inevitably increases the reliability of diagnostic parameters, which is calculated based on these results.

However, it must be said that these findings and results can be more inclusive and contain more sequences in the quantitative validation process. It should, also, be noted that the most delicate phase in the use of our approach is the form of modeling phase. This phase, which is based on a manual process, influences largely on the quality of results. It must, therefore, be carried out carefully with the help of a domain expert.

VI. CONCLUSION

In this article, we proposed a new automatic method of brain images segmentation based on the AC model to extract the Hippocampus and the CC. Our contribution is to combine the geometric and statistical method of the AC. The evolution of the contour is based on the geometry and some priori knowledge such as surface and standard deviation. We find that our method Modify Level set give a good result. We can improve our work by adding a classification step. We can use the method of classification Support Vector Machine. With the two areas Hippocampus and CC, we can diagnose Alzheimer diseases.

REFERENCES

P. Aljabar, R.A. Heckemann, A. Hammers, J.V. Hajnal, and D. Rueckert, Multi-atlas based segmentation of brain images: Atlas selection and its effect on accuracy, Neuroimage 46 (2009), 726–738.

E. Aminoff, N. Gronau, and M. Bar, The parahippocampal cortex mediates spatial and nonspatial associations, Cereb Cortex 17 (2007), 1493–1503.

A. Andreopoulos and J. Tsotsos, Efficient and generalizable statistical models of shape and appearance for analysis of cardiac MRI, Med Image Anal (2008), 335–357.

B.A. Ardekani and A.H. Bachman, Model-based automatic detection of the anterior and posterior commissures on MRI scans, Neuroimage 46 (2009), 677–682.

J. Atif, O. Nempont, O. Colliot, E. Angelini, and I. Bloch. Level Set Deformable Models Constrained by Fuzzy Spatial Relations. In Information Processing and Management of Uncertainty in Knowledge-Based Systems, IPMU, France, 2006, pp. 1534–1541.

H. Aymeric, and C.M. Christine, Détection robuste et automatique des contours myocardiques sur des séquences IRM cardiaques marquées, GRETSI (2005).

K.O. Babalola, B. Patenaude, P. Aljabar, J. Schnabel, D. Kennedy, W. Crum, S. Smith, T. Cootes, M. Jenkinson, and D. Rueckert, An evaluation of structures in the brain, Neuroimage 47 (2009), 1435–1414 47.

M. Bar and E. Aminoff, Cortical analysis of visual context, Neuron 38 (2003), 347–358.

B. Bascle. Contributions et applications des modèles déformables en vision par ordinateur. Thèse de doctorat, université de Nice-sophia antipolis, 1994.

M.F. Bear, F.W. Connors, and M.A. Paradiso. Chapitre 1 : Neurosciences - à la découvertes du cerveau. Edditions Pradel. 2007.

J. Bollinger, M.T. Rubens, E. Masangkay, J. Kalkstein, and A. Gazzaley, An expectation-based memory deficit in aging, Neuropsychologia 49 (2011), 1466–1475.

R.L. Buckner, J.R. Andrews-Hanna, and D.L. Schacter, The brain's default network: anatomy, function, and relevance to disease, Ann N Y Acad Sci 11 (2008), 1–38.

L. Caselles, F. Catt, C. Coll et, and F. Dibos, A geometric model for active contours in image processing, Numer Math (1993), 1–31.

V. Caselles, R. Kimmel, and G. Sapiro, Geodesic Active Contours, Int J Comput Vis 22 (1997), 61–79.

T. Chan and L. Vese, Active contours without edges, IEEE Trans Image Process 10 (2001), 266–277.

M.A. Charmi, S. Derrode, and F. Ghorbel, Fourier-based geometric shape prior for snakes, Pattern Recognit Lett 29 (2008), 897–904.

C.H. Chen and G.G. Lee, Image Segmentation Using Multiresolution Wavelet Analysis and Expectation-Maximization (EM) Algorithm for Digital Mammography, Int J Imaging Syst Technol 8 (1997), 491–504.

W. Chen and M.L. Giger. A fuzzy c-means (FCM) based algorithm for intensity inhomogeneity correction and segmentation of MR images. IEEE International Symposium on Biomedical Imaging, Arlington, VA, 2004, pp. 1307-1310.

S. Chen and R.J. Radke. Level set segmentation with both shape and intensity priors. 12th IEEE International Conference on Computer Vision, Japan, 2009, pp.763-770.

T.F. Cootes and C.J. Taylor, Combining point distribution models with shape models based on finite element analysis, BMVC94 2 (1994), 419–428.

H. Delingette and J. Montagnat, Shape and topology constraints on parametric active contours, Comput Vis Image Understanding 83 (2001), 140–171.

B.C. Dickerson, E. Feczko, J.C. Augustinack, J. Pacheco, J.C. Morris, B. Fischl, and R.L. Buckner, Differential effects of aging and Alzheimer's disease on medial temporal lobe cortical thickness and surface area, Neurobiol Aging 30 (2009), 432–440.

H. M. Duvernoy. The Human Hippocampus: Functional Anatomy, Vascularization and Serial Sections with MRI. The Human Hippocampus, Springer, 2005.

S. Ettaieb, K. Hamrouni, and S. Ruan. Statistical models of shape and spatial relation-application to hippocampus segmentation. 9th International Conference on Computer Vision Theory and Applications (Visapp), Lisbon-Portugal, Janvier, 2014.

R. Epstein, A. Harris, D. Stanley, and N. Kanwisher, The parahippocampal place area: recognition, navigation, or encoding, Neuron 23 (1999), 115–125.

M Kayalvizhi, G Kavitha, and CM Sujatha, Analysis of ventricle regions in Alzheimer's brain MR images using level set based methods, International Journal of Biomedical Engineering and Technology 12, 300–319.